3 Biotech (2023) 13:312
https://doi.org/10.1007/s13205-023-03721-w

ORIGINAL ARTICLE

# Silencing of purinergic receptor P2Y2 inhibited enteric neural crest cell proliferation, invasion and migration via suppressing ERK signaling pathway in Hirschsprung disease

Dengrui Liu[1] · Hongxia Kang[2] · Mingtai Gao[1] · Wei Pei[1] · Shimo Wang[1] · Zhou Chen[1]

Received: 6 April 2023 / Accepted: 29 July 2023 / Published online: 23 August 2023


## Abstract

The current study aimed to explore the effect and underlying mechanism of the purinergic receptor P2Y2 in regulating the loss of intestinal neurons and the intestinal neural crest in Hirschsprung's disease (HSCR). Western blotting was used to assess the expression levels of P2Y2 in colon tissues. An in vivo HSCR mouse model was established following treatment with benzalkonium chloride (BAC). We overexpressed or silenced P2Y2 in SH-SY5Y cells, and cell proliferation, migration, and invasion were subsequently investigated by CCK-8, wound healing, and transwell assays, respectively. Additionally, we implemented a xenograft model to assess the impact of P2Y2 on tumor growth as well as the expression of extracellular signal-regulated kinase (ERK). The results showed that the expression of P2Y2 protein in the colon tissues of patients with HSCR was lower than that in the normal colon tissues. P2Y2 expression is downregulated in the colon tissues of mice with HSCR. Additionally, P2Y2 silencing inhibited SH-SY5Y cell proliferation, invasion, and migration. Furthermore, adenosine 5′-triphosphate (ATP, a strong agonist of P2Y2)-induced P2Y2 overexpression enhanced the proliferation, invasion, and migration of SH-SY5Y cells. Immunofluorescence staining and western blot analysis revealed that P2Y2 silencing downregulated phosphorylated (p)-ERK in SH-SY5Y cells. In addition, treatment with PD98059, a p-ERK inhibitor, reversed the effects of ATP on SH-SY5Y cell proliferation, invasion, and migration. Finally, we demonstrated that P2Y2 silencing suppressed tumor growth and decreased p-ERK expression. Overall, the results of the present study suggest that P2Y2 plays an important role in HSCR pathogenesis. P2Y2 silencing inhibited the proliferation, invasion, and migration of nerve cells by suppressing the ERK signaling pathway. P2Y2 silencing could be considered an innovative and possible target for treating HSCR.

**Keywords** P2Y2 · ERK · Hirschsprung disease · SH-SY5Y cells

## Introduction

Congenital megacolon, also known as Hirschsprung's disease (HSCR), is a congenital disease of the digestive tract caused by functional defects of the enteric nervous system (ENS) during embryonic development (Kessmann 2006). The incidence of HSCR is estimated to be one case per 200–5000 live births (Pan and Li 2007). A previous study suggested that HSCR could be caused by the absence of ENS and the inhibition of enteric neural crest cell (ENCC) migration, thus resulting in the deficiency of ganglia in the distal intestinal wall, spastic narrowing of the distal intestinal segment and dilation of the proximal colon (Tam and Garcia-Barcelo 2004). The main clinical symptoms of HSCR include constipation, vomiting, bloating, and growth disorder. Untreated children usually die of intestinal inflammation or perforation. Emerging evidence suggests that HSCR results from interactions between multiple genes. However, genetic studies can only explain a limited number of HSCR cases. Therefore, the pathogenesis remains unclear. The neural crest is a provisional structure formed during early development of vertebrate embryos (Bronner and Simões-Costa 2016). A previous study demonstrated that

✉ Dengrui Liu
Liujiaxia2005@163.com

[1] Department of Pediatric Surgery, The First Hospital of Lanzhou University, No. 1 Donggang West Road, Lanzhou 730000, Gansu, China

[2] Department of Pain, Gansu Provincial People's Hospital, Lanzhou 730000, Gansu, China

ENCCs can differentiate into different types of cells, such as enteric nervous cells, through their migration and proliferation (Burns 2005). Therefore, abnormalities in ENCC development may result in the onset of distal intestinal ganglion disease (Lake and Heuckeroth 2013).

As a neurotransmitter, adenosine 5′-triphosphate (ATP) is involved in the differentiation, migration, and survival of neuronal cells (Fields 2011; Agresti et al. 2005). Interestingly, the biological role of ATP depends on its receptors (Lalo et al. 2011). Two types of ATP receptors, P1 and P2, have been identified. P2 receptors are divided into the P2X and P2Y subtypes. To date, eight subtypes of P2Y have been identified. Among these subtypes, the purinergic receptor P2Y2 (P2Y2) is widely distributed in gastrointestinal tract (Burnstock 2007). A previous study showed that P2Y2 receptors are mainly involved in the regulation of muscle relaxation in the ENS (Liu et al. 2015). More specifically, P2Y2 regulates muscle relaxation in the ENS, while P2Y2 inhibition results in impaired relaxation of the intestinal canal (Liu et al. 2015). Furthermore, the expression of P2Y1 and P2Y2 is downregulated in the aganglionic gut of HSCR (Od and Puri 2008). However, the current knowledge on the role and molecular mechanisms of P2Y2 in the development of HSCR remains limited. Extensive research has indicated that P2Y2 plays a biological role by regulating the ERK signaling pathway. Nucleotides stimulate P2Y2 to activate ERK1/2 through a mechanism dependent on PKC and phospholipase D (Kudirka et al. 2007). P2Y2 promotes fibroblast activation and skeletal muscle fibrosis via the ERK signaling pathway (Chen et al. 2021). Moreover, synergy between P2Y2 and the ERK signaling pathway is essential for HeLa cell proliferation and c-Fos expression (Muscella et al. 2003). Therefore, we hypothesized that P2Y2 plays a role in regulating HSCR through the ERK signaling pathway.

In the current study, a benzalkonium chloride (BAC)-induced HSCR model was established in mice and SH-SY5Y cells to investigate the role and regulatory mechanism of P2Y2 in the development of HSCR.

## Methods and materials

### Tissue collection

Thirty specimens of colon tissue (15 specimens from HSCR cases and 15 from matched control subjects) were intraoperatively collected from patients at The First Hospital of Lanzhou University, and then snap frozen in liquid nitrogen, and stored at − 80 °C until use. The diagnosis of HSCR was confirmed by pathological examination. All study participants were required to provide written informed consent prior to enrollment. The study protocol was reviewed and approved by the Institutional Review Board of the First Hospital of Lanzhou University (approval no. LDYYLL2021-69). This study was conducted in accordance with the guidelines of the Declaration of Helsinki.

### Animals

Sixteen BALB/c mice and 12 BALB/c nude mice (SPF grade; age, 3–4-month-old; weight, 24–33 g) were purchased from Chengdu Dossy Experimental Animals Co., Ltd. (Chengdu, Sichuan). Mice were maintained on a 12-h light/dark cycle at a temperature of 25 ± 1 °C and relative humidity of 50–60%. All the mice had free access to food and water. The animal experiments were approved by the Ethics Committee of the First Hospital of Lanzhou University (approval no. LDYYLL2022-252). All animal experiments were performed in accordance with the principles of the Declaration of Helsinki.

### HSCR mouse model and treatment

The construction of the HSCR model was based on previous studies (Hu et al. 2019; Yoneda et al. 2002). Mice were randomly allocated into two different groups using the random number table method: the control ($n = 8$) and HSCR model groups ($n = 8$). To establish the HSCR model, the mice were treated with BAC. Briefly, mice were anesthetized by intraperitoneal injection of pentobarbital sodium (30 mg/kg), and laparotomy was performed with a midline incision. Subsequently, the sigmoid colon was excised from the abdomen. A small cut was made in the avascular area of the sigmoid mesentery and a filter paper strip (dimensions, 0.8 cm × 1 cm) soaked with 0.1% BAC (MilliporeSigma) was placed within 1–2 cm of the colon. To avoid dehydration, the filter paper was soaked in 100 µL of 0.1% BAC solution every 5 min for a total of 15 min. Subsequently, the filter paper strip was removed and the colon was washed with 0.9% saline. The mice in the control group were treated with 0.9% saline using the same method. The wound was sutured using silk thread and disinfected with iodophor. Stenosis, dilation, and stool retention were observed in BAC-treated segments of the gut and colon. At the end of the experiments, the mice were euthanized immediately following sedation with 1% sodium pentobarbital (30 mg/kg) via tail vein injection. Euthanasia was performed by $CO_2$ asphyxiation at a flow rate of 30% volume/min of gas displacement in a chamber for 5 min according to the revised AVMA guidelines (December 2020). The death of animals was verified when they failed to respond to mild stimulation using a platinum wire (Offenburger and Ho 2018). Colon tissues, including the dilated and stenotic colon segments, were isolated and stored at − 80 °C for further analysis.

### Histological analysis and hematoxylin and eosin (H&E) staining

Colon tissues were fixed in 4% paraformaldehyde for 24 h prior to embedding in paraffin. Colon tissues were subjected to histopathological analysis via hematoxylin and eosin (H&E) staining, as previously described (Zhang et al. 2015).

### Immunohistochemical (IHC) staining

The paraffin blocks were sectioned to a thickness of 4 μm. IHC staining was then performed to detect the protein expression levels of P2Y2 in the colon or tumor tissues of mice, according to the manufacturer's protocol (Li et al. 2020).

### Cell culture

Human SH-SY5Y cells were obtained from ProCell (Wuhan, China) and identified using short tandem repeat (STR) analysis. The cells were maintained in DMEM supplemented with 10% FBS at 37 °C in a humidified incubator with 5% $CO_2$. SH-SY5Y cells at a density of 105 cells/well were transfected with normal control (NC) small interfering RNA (siRNA) or P2Y2 siRNA using Lipofectamine® 3000 (Invitrogen; Thermo Fisher Scientific, Inc.), according to the manufacturer's instructions. To induce P2Y2 expression and inhibit the activity of the extracellular signal-regulated kinase 1/2 (ERK1/2) signaling pathway, SH-SY5Y cells were treated with 100 μM ATP (Sigma Aldrich, USA), a strong agonist of P2Y2, and 10 μM PD98059 (Cell Signaling Technology, USA), an ERK1/2 inhibitor.

### Cell counting kit 8 (CCK-8) assay

The viability of SH-SY5Y cells was assessed using the CCK-8 assay (Thermo Fisher Scientific, Inc., USA), according to the manufacturer's instructions (Zeng et al. 2020). The absorbance at 450 nm was measured using a microplate reader.

### Wound healing assay

A wound healing assay was performed to assess the migration ability of SH-SY5Y cells. Briefly, SH-SY5Y cells were grown in 96-well plates until they reached confluence. Subsequently, the cell monolayer was scraped with a 200-μL pipette tip. The old medium was replaced with fresh medium, and the cells were grown continuously. The exfoliated cells were removed by washing with the culture medium. The width between the two edges of the wound was calculated. The wounds in each hole were observed in multiple randomly selected visual fields. After incubation for 24 h, the wound width was measured. The scratched areas were quantified using the ImageJ software (NIH). The relative wound recovery ratio was calculated using the following formula: relative wound recovery ratio (%) = [distance within scratch (0 h) − distance within scratch (24 h)]/distance within scratch (0 h).

### Transwell assay

The invasion capacity of the cells was assessed using the Transwell assay. Briefly, SH-SY5Y cells were resuspended in DMEM at a density of $1 \times 10^5$ cells/mL, and 200 μL of cell suspension/well was plated into the upper chambers of a 24-well Transwell plate. The lower chamber was filled with 600 μL DMEM supplemented with 10% FBS (HyClone, Cytiva). The cells were cultured for 48 h at 37 °C in an incubator with 5% $CO_2$. Finally, cells were fixed with 4% paraformaldehyde for 20 min and stained with 0.1% crystal violet for 15 min. Invading cells were observed under an inverted microscope in five randomly selected fields (Olympus Corporation, Japan).

### Immunofluorescence (IF) staining

IF staining was performed as previously described (Yan et al. 2021). SH-SY5Y cells were fixed in 4% paraformaldehyde for 20 min at room temperature, washed with PBS, and permeabilized with Triton X-100 for 10 min at room temperature. After cooling to room temperature, SH-SY5Y cells were washed with 0.1 mol/L PBS and blocked with 5% BSA at room temperature for 1 h. Subsequently, cells were incubated with primary antibodies against phosphorylated (p)-ERK1/2 at 4 °C overnight. The following day, cells were incubated with the corresponding secondary antibodies at 37 °C for 30 min. Finally, the cell nuclei were labeled with 4′,6-diamidino-2-phenylindole (DAPI; cat. no. ZLI-9557; ZSGB-BIO Technology Co., Ltd.) at room temperature for 10 min and the stained cells were observed under a fluorescence microscope.

### RNA extraction and reverse transcription-quantitative PCR (RT-qPCR).

Total RNA was extracted using TRIzol® reagent (Thermo Fisher Scientific, Inc., USA) and then reverse-transcribed into cDNA using a reverse transcription kit (Invitrogen; Thermo Fisher Scientific, Inc., USA). The relative expression levels of target genes were assessed by RT-qPCR using the SYBR Premix Ex Taq kit (Bao Biological Engineering, Co., Ltd., China). Expression levels were calculated using the $2^{-\Delta\Delta Cq}$ method. The primer sequences used were as follows: For P2Y2, forward, 5′-CTC ATT TGG CAG GGA CTC AGG-3′, and reverse, 5′-AAT GGC AGC TGT TTG

CAT GG-3′; and β-actin, forward, 5′-GGA GAT TAC TGC CCT GGC TCC TA-3′, and reverse, 5′-GAC TCA TCG TAC TCC TGC TTG CTG-3′.

### Western blot analysis

SH-SY5Y cells were lysed using a RIPA buffer (Cell Signaling Technology, Inc., USA). Protein concentration was measured using a BCA kit (Millipore Sigma, USA). Total protein extracts (30 µg/sample) were separated using 10% SDS-PAGE and transferred onto nitrocellulose membranes. Subsequently, the membranes were blocked with 5% nonfat milk and incubated with primary antibodies against P2Y2 (cat. no. ab272891, Abcam, USA; dilution, 1/500), p-ERK1 (phosphorylated at T202)/2 (phosphorylated at T185) (cat. no. ab201015 Abcam, USA, dilution, 1/1000), ERK1/2 (cat. no. ab184699 Abcam, USA; dilution, 1/10,000) and β-actin (cat. no. BM0627; Boster Biological Technology, Ltd., China; dilution, 1/1000). The membrane was washed with Tris-buffered saline/0.1% Tween (TBST), followed by incubation with HRP Goat anti-rabbit IgG (cat. no. ab6721, Abcam, USA) for 1.5 h. The bands were visualized using an ECL system (Affinity Biosciences), and β-actin served as an internal control.

### Tumor formation assay in vivo

BALB/c nude mice were randomly divided into two groups ($n=6$ each): sh-RNA-NC and shRNA-P2Y2. SH-SY5Y cells transfected with shRNA-P2Y2 or control were collected and re-suspended in medium at a concentration of $1\times10^6$ cells/mL, and 200 µL of the cell suspension was injected into the flank of nude mice. Tumor diameter was measured using a Vernier caliper. 21 days after successful establishment of the model, all mice were anesthetized with 1% sodium pentobarbital (30 mg/kg) via tail vein injection and euthanized by carbon dioxide inhalation. The tumor tissue was removed and kept at − 80 °C for subsequent analysis. Tumor volume was calculated using the formula: $V=1/2\times L\times D^2$ (where $L$ represents the largest diameter measured and $D$ represents the smallest diameter measured).

### Statistical analysis

All data are expressed as mean ± standard deviation (SD). All statistical analyses were carried out using SPSS 20.0 (IBM Corp.) software. Differences among multiple groups were compared using one-way ANOVA followed by Tukey's post hoc test. $P<0.05$ was considered to indicated a statistically significant.

## Results

### Expression of P2Y2 in HSCR colon tissues

As shown in Fig. 1a, the levels of P2Y2 protein in the colon tissues of HSCR patients were clearly decreased compared with their levels in the paired normal colon tissues. The quantitative results of western blotting showed the same result (Fig. 1b, $1.001\pm0.057$ vs. $0.242\pm0.104$, $P<0.01$). IHC results showed that the expression of P2Y2 in the colon tissue of patients with HSCR was significantly decreased (Fig. 1c), and the number of P2Y2 positive cells was significantly reduced compared to that in the control group (Fig. 1d, $5.285\pm0.879$ vs. $2.077\pm0.311$, $P<0.01$). Moreover, to determine the expression levels of P2Y2 in HSCR, an HSCR mouse model was established following treatment with BAC. As shown in Fig. 1e, fewer ganglion cells were observed in the dilated HSCR colon and stenotic intestinal tissues than in the normal colon tissues (Fig. 1e). The relative protein and mRNA expression levels of P2Y2 in the control and HSCR groups were determined using IHC and RT-qPCR analyses. IHC results indicated that, compared with normal colon tissues, P2Y2 protein was downregulated in the colon tissues of mice in the HSCR group (Fig. 1f). More importantly, the protein levels of P2Y2 in stenotic colon tissue were notably lower than those in the dilated segment of colon tissue (Fig. 1f). The quantification results of IHC staining showed that, compared with the control group, the number of P2Y2 positive cells was significantly decreased in the colon tissues of the HSCR model group ($0.321\pm0.005$ vs. $0.289\pm0.002$, $P<0.05$), and the decrease in stenotic colon (SC) was significantly greater than that in the transitional colon (TC, Fig. 1g, $0.289\pm0.002$ vs. $0.261\pm0.002$, $P<0.05$). RT-qPCR results further supported this observation (Fig. 1h, $1.01\pm0.145$ vs. $0.81\pm0.036$, $P<0.01$, $0.81\pm0.036$ vs. $0.61\pm0.053$, $P<0.05$,).

### P2Y2 silencing attenuates SH-SY5Y cell proliferation, migration and invasion

We evaluated the effect of P2Y2 on SH-SY5Y cell development. As shown in Fig. 2a, b, the mRNA (Fig. 2a, $1.003\pm0.112$ vs. $0.750\pm0.125$, $P<0.01$) and protein expression levels of P2Y2 (Fig. 2b) were significantly reduced in P2Y2-depleted SH-SY5Y cells ($1.000\pm0.019$ vs. $0.289\pm0.025$, $P<0.01$), which were further enhanced following treatment with ATP ($0.750\pm0.125$ vs. $0.96\pm0.128$, $P<0.05$, $0.289\pm0.025$ vs. $0.994\pm0.007$, $P<0.01$). The CCK-8 assay demonstrated that the proliferative ability of SH-SY5Y cells was suppressed by P2Y2

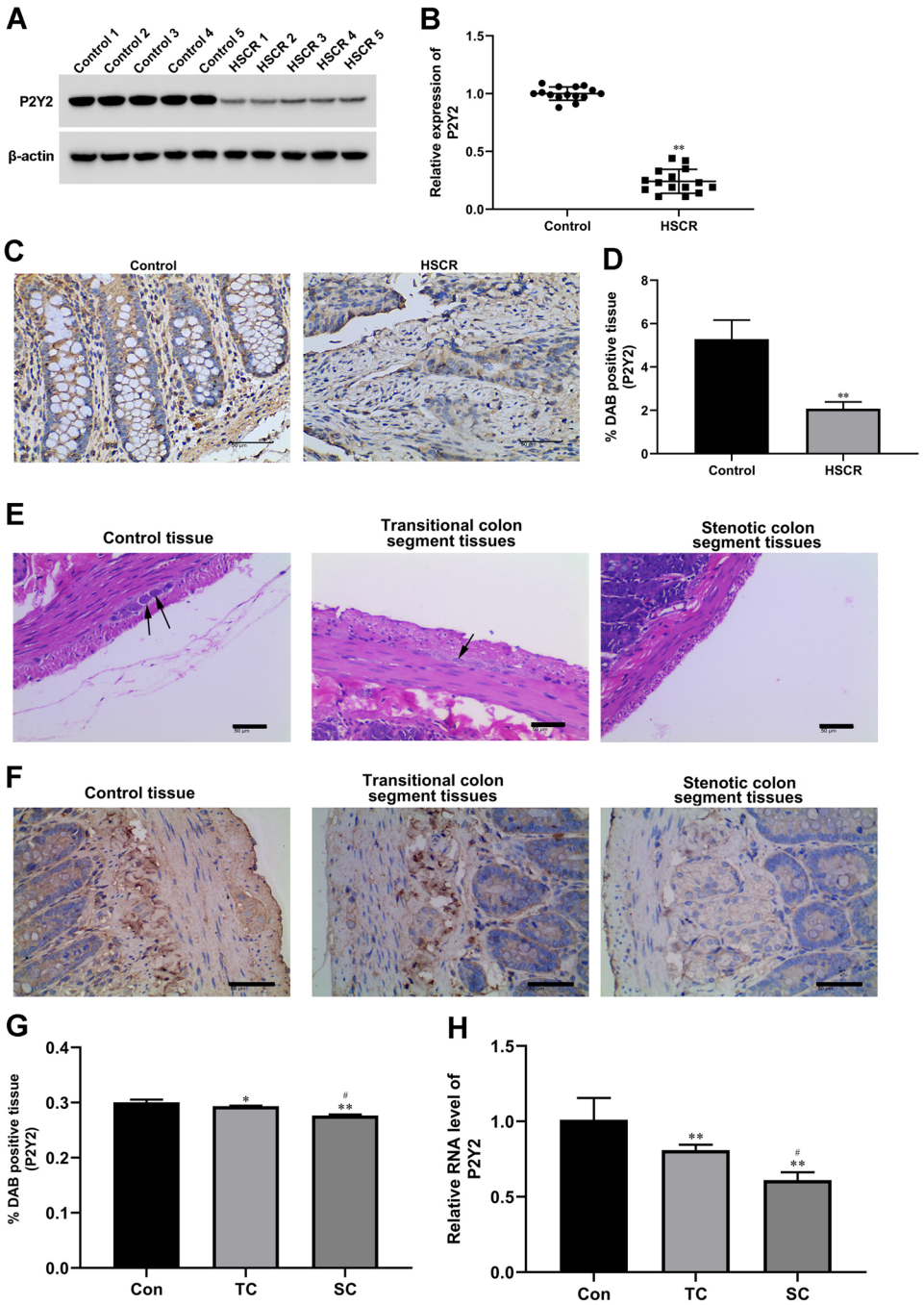


**Fig. 1** Downregulated P2Y2 in HSCR colon tissues. **a–d** Thirty specimens of colon tissues (15 specimens from HSCR patients and 15 specimens from matched control subjects) were collected. Western blot and immunohistochemistry (IHC) stain were used to detect the levels of P2Y2 expression in colon tissues. The expression of P2Y2 in the colon tissues was decreased compared with normal colon tissues. **e** 12 Balb/c mice were randomly divided into 2 groups, namely the control group and the HSCR model group. Benzalkonium chloride (BAC) treatment was performed to build up the HSCR mouse model. Hematoxylin and eosin (H&E) stained images of mouse colon tissues (×400). The arrow points to ganglion cells. Fewer ganglion cells were observed in the dilated HSCR colon and stenotic intestinal tissues compared with normal colon tissues. **f** The expression of P2Y2 was tested using IHC stain. The positive immunohistochemical reaction was visualized as brown. **g** The quantification result of IHC stain. The number of P2Y2 positive cells in the stenotic colon tissue was lower compared with those in the dilated segment of the colon tissue. **h** The expression of P2Y2 mRNA level was detected in the HSCR group and the control group using RT-qPCR. Compared with the control group, the expression of P2Y2 was decreased in the colon tissues of the HSCR model group, and the decrease in SC was greater than that in TC. *Con* control, *TC* transitional colon segment tissues, *SC* stenotic colon segment tissues. All experiments were performed in 6 replicates and presented as mean ± SE. $^{*}P < 0.05$ vs. Con, $^{**}P < 0.01$ vs. Con, $^{\#}P < 0.05$ vs. TC

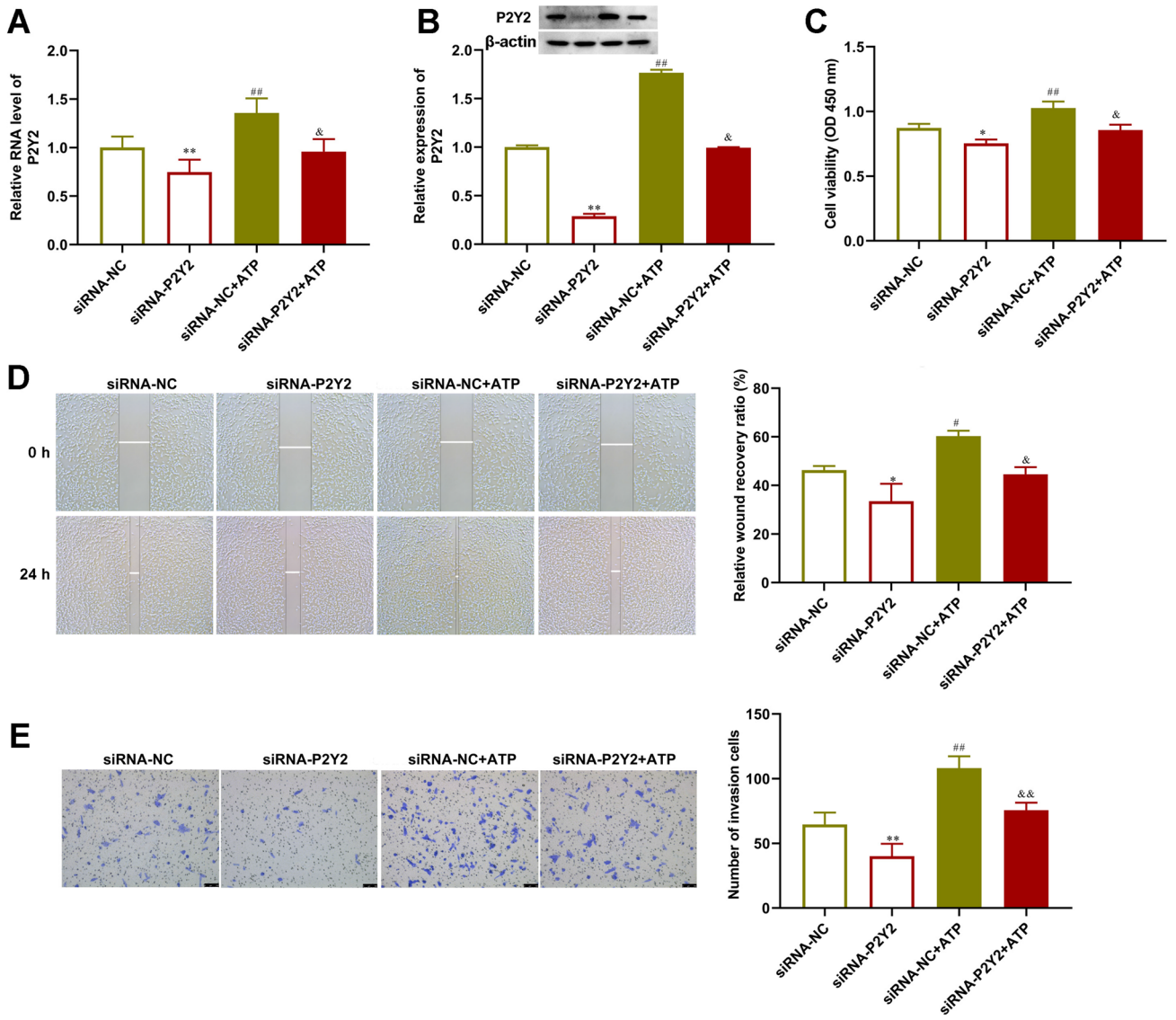


**Fig. 2** Silencing of P2Y2 inhibited SH-SY5Y cell proliferation, migration, and invasion. Normal control (NC) siRNA or P2Y2 siRNA were transfected into SH-SY5Y cells ($1.0\times10^5$/cm$^2$) using Lipofectamine 3000. 100 μM adenosine 5′-triphosphate adenosine triphosphate (ATP, a strong agonist for P2Y2) was used to co-treat SH-SY5Y cells ($1.0\times10^5$/cm$^2$). Cells were analyzed for mRNA levels 48 h after transfection. **a** The mRNA expression of P2Y2 was tested by RT-qPCR. The mRNA level of P2Y2 were reduced in P2Y2-depleted SH-SY5Y cells. **b** The protein expression of P2Y2 was detected using Western blot analysis. The expression of P2Y2 was decreased in P2Y2-depleted SH-SY5Y cells. **c** Cell viability of SH-SY5Y cells was tested by CCK-8 assay. The proliferation ability of SH-SY5Y cells was suppressed by P2Y2 silencing, which was restored by ATP. **d** SH-SY5Y cell migration was detected by Wound-healing assay. The wound recovery ratio was reduced in P2Y2-depleted cells, which was abrogated by ATP. **e** Transwell assay was used to examine SH-SY5Y cell invasion. The number of invasion cells was decreased in P2Y2-depleted cells, which was reversed by ATP. All experiments were performed in triplicate and presented as mean ± SE. $^{*}P<0.05$ vs. Con, $^{**}P<0.01$ vs. Con, $^{\#}P<0.05$ vs siRNA-NC, $^{\#\#}P<0.01$ vs siRNA-NC, $^{\&}P<0.05$ vs siRNA-P2Y2, $^{\&\&}P<0.01$ vs siRNA-P2Y2

silencing ($0.873\pm0.031$ vs. $0.755\pm0.029$, $P<0.05$), which was restored by ATP (Fig. 2c, $0.755\pm0.029$ vs. $0.856\pm0.042$, $P<0.05$). Both the wound recovery ratio (Fig. 2d, $46.296\pm1.652$ vs. $33.472\pm7.160$, $P<0.05$) and the number of invasive cells (Fig. 2e, $64.667\pm9.158$ vs. $40.000\pm9.654$, $P<0.01$) were reduced in P2Y2-depleted cells, suggesting that P2Y2 knockdown attenuated cell migration and invasion (Fig. 2d, e). As expected, cell treatment with ATP abrogated P2Y2 silencing-mediated impaired migration (Fig. 2d, $33.472\pm7.160$ vs. $44.571\pm2.898$, $P<0.05$) and invasion (Fig. 2e, $40.000\pm9.654$ vs. $75.667\pm5.785$, $P<0.01$) of SH-SY5Y cells.

## P2Y2 regulates the phosphorylation levels of ERK1/2 in SH-SY5Y cells

We next investigated whether P2Y2 promotes the activation of ERK1/2 signaling. Western blot analysis indicated that P2Y2 silencing significantly downregulated total ERK1/2 and p-ERK1/2 levels in cells transfected with siRNA clones targeting P2Y2 (Fig. 3a). By contrast, ATP-induced P2Y2 overexpression enhanced the expression of both total ERK1/2 and p-ERK1/2 (Fig. 3a). The quantitative results of western blotting also suggested that the levels of p-ERK1/2 (Fig. 3b) and ERK1/2 (Fig. 3c) were inhibited by P2Y2 silencing ($1.000 \pm 0.015$ vs. $0.399 \pm 0.054$, $P < 0.01$, $1.000 \pm 0.039$ vs. $0.584 \pm 0.033$, $P < 0.01$) and further promoted by co-treatment with ATP ($0.399 \pm 0.054$ vs. $0.926 \pm 0.033$, $P < 0.01$, $0.584 \pm 0.033$ vs. $1.012 \pm 0.095$, $P < 0.01$, $P < 0.01$). In addition, the IF assay revealed that P2Y2 silencing inhibited the translocation of activated p-ERK1/2 from the cytoplasm to the nucleus (Fig. 3d; $14.765 \pm 0.324$ vs. $12.537 \pm 0.638$, $P < 0.01$). The opposite effect was observed in ATP-treated SH-SY5Y cells (Fig. 3d, $12.537 \pm 0.638$ vs. $17.181 \pm 0.305$, $P < 0.01$).

## ERK1/2 inhibition attenuates SH-SY5Y cell development induced by P2Y2 overexpression

Finally, the present study explored the possible molecular mechanism underlying the effect of P2Y2 on SH-SY5Y cell development through P2Y2 receptors. The results showed that the inhibition of ERK1/2 activity using PD98059

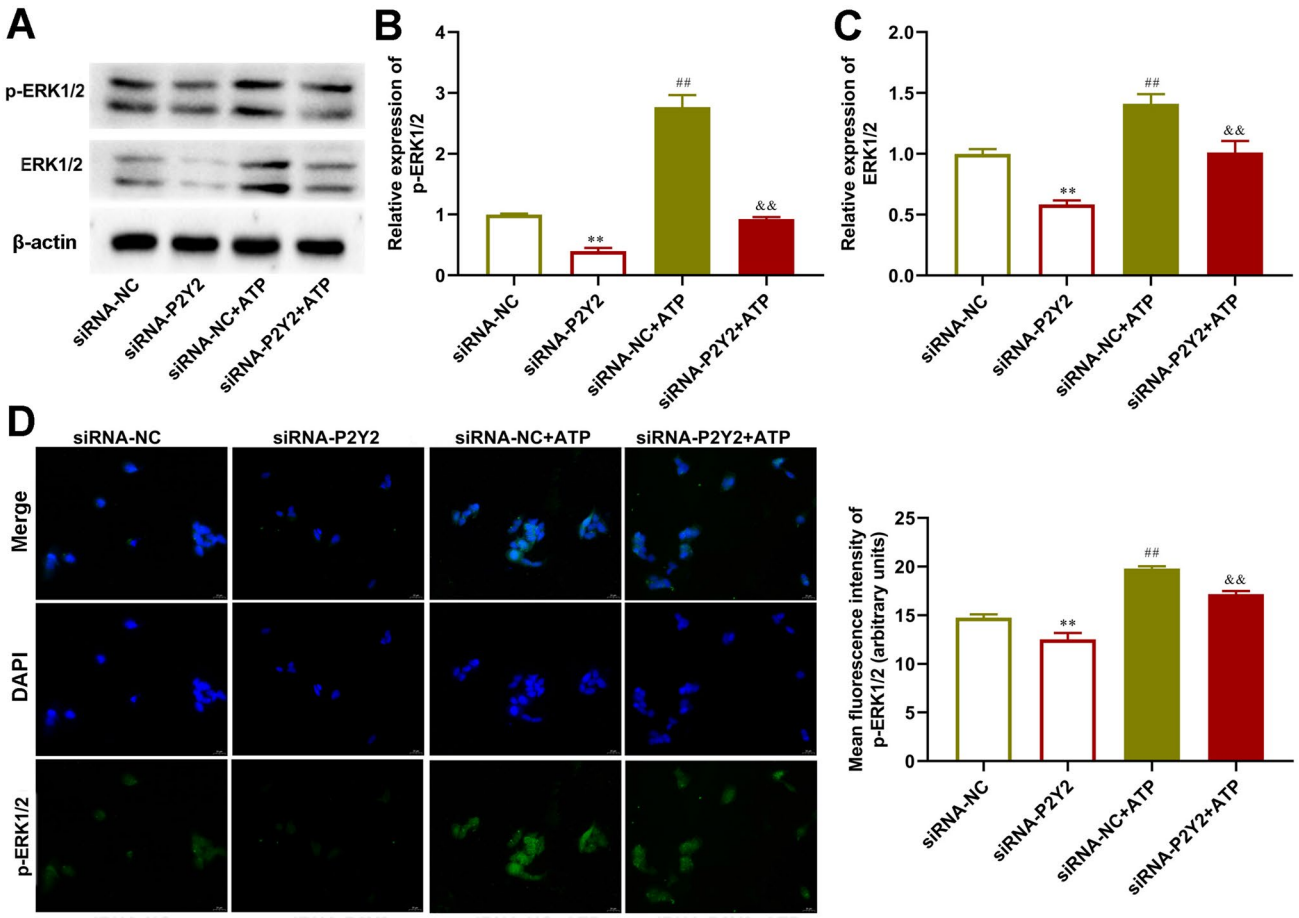


**Fig. 3** P2Y2 regulated ERK1/2 phosphorylation level in SH-SY5Y cells. Normal control (NC) siRNA or P2Y2 siRNA were transfected into SH-SY5Y cells ($1.0 \times 10^5/cm^2$) using Lipofectamine 3000. 100 μM adenosine 5′-triphosphate adenosine triphosphate (ATP) was used to strengthen P2Y2 in SH-SY5Y cells ($1.0 \times 10^5/cm^2$). Cells were analyzed for protein expression levels 48 h after transfection. **a–c** The protein expression of ERK1/2 and p-ERK 1/2 was tested using Western blot analysis. The level of p-ERK1/2 and ERK1/2 was inhibited by P2Y2 silencing and was further promoted by co-treated of ATP. **d** The spatial expression of p-ERK 1/2 was assayed by immunofluorescence (IF). P2Y2 silencing inhibited the translocation of activated p-ERK1/2 from the cytoplasm to the nucleus. The opposite effect was observed in ATP-mediated SH-SY5Y cells. All experiments were performed in triplicate and presented as mean ± SE. $^{*}P < 0.05$ vs. Con, $^{**}P < 0.01$ vs. Con, $^{\#}P < 0.05$ vs siRNA-NC, $^{\#\#}P < 0.01$ vs siRNA-NC, $^{\&}P < 0.05$ vs siRNA-P2Y2, $^{\&\&}P < 0.01$ vs siRNA-P2Y2

abolished the effect of P2Y2 overexpression on SH-SY5Y cell proliferation (Fig. 4a, $0.991 \pm 0.042$ vs. $0.941 \pm 0.033$, $P < 0.05$). Moreover, the scratch migration assay showed that ATP enhanced the wound recovery ratio (Fig. 4b; $66.606 \pm 3.868$ vs. $54.713 \pm 3.061$, $P < 0.01$) and promoted SH-SY5Y cell migration (Fig. 4c), which was inhibited by PD98059. Cell counting results of the transwell invasion assay (Fig. 4d) and representative images of the transwell invasion assay (Fig. 4e) showed that cell invasion ability was enhanced in SH-SY5Y cells treated with ATP ($72.000 \pm 11.437$ vs. $116.000 \pm 11.541$, $P < 0.01$), but the effect was reversed by co-treatment with PD98059 ($116.000 \pm 11.541$ vs. $91.500 \pm 12.178$, $P < 0.01$). These findings indicate that P2Y2 overexpression promoted SH-SY5Y cell development by enhancing the ERK1/2 signaling pathway.

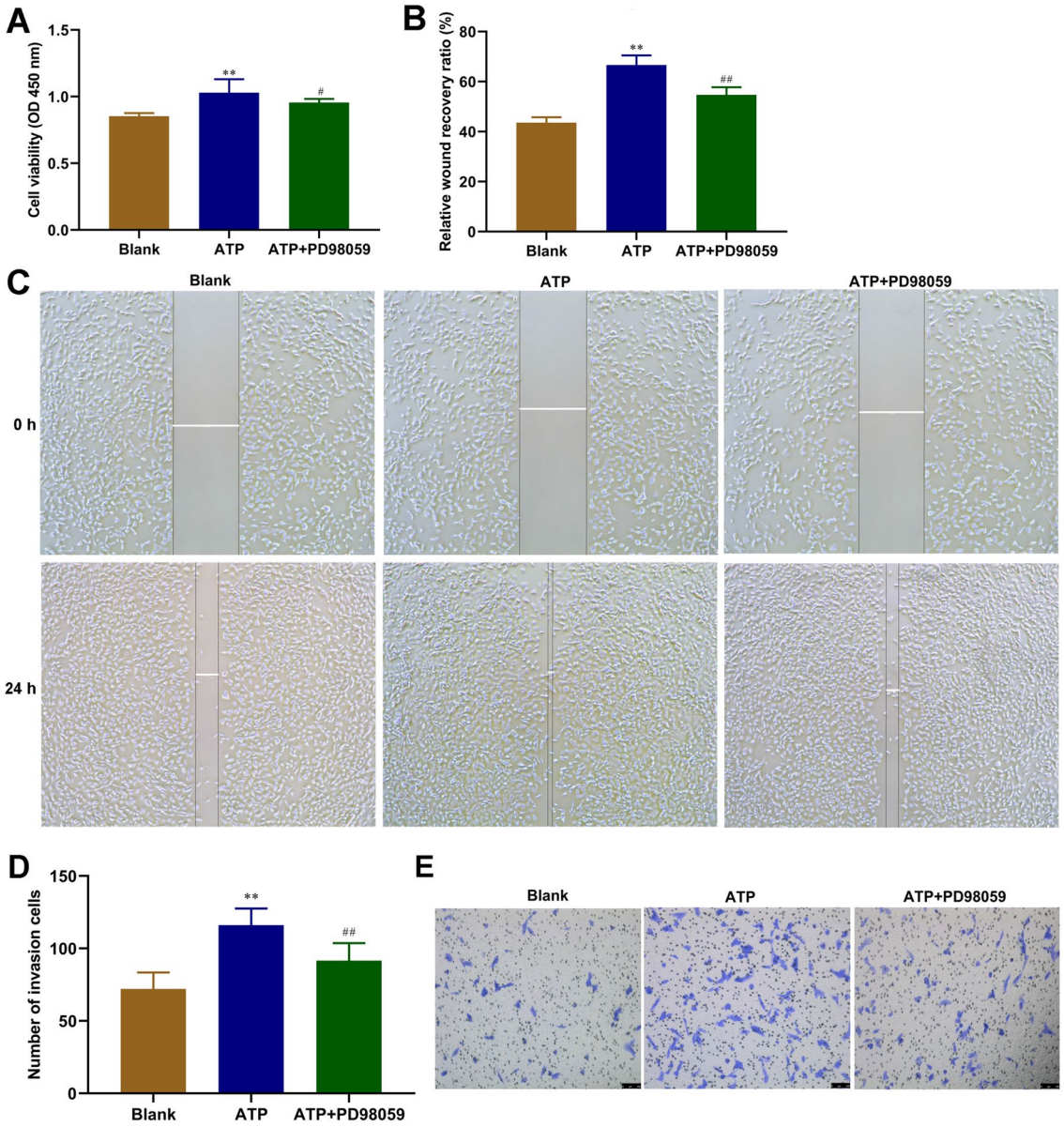


**Fig. 4** Inhibition of ERK1/2 reduced SH-SY5Y cell development induced by P2Y2 overexpression. To promote P2Y2 expression and inhibit the activity of ERK1/2 signaling pathway, adenosine 5′-triphosphate adenosine triphosphate (ATP, a strong agonist for P2Y2, 100 μM) and ERK1/2 inhibitor PD98059 (10 μM) were used to treat SH-SY5Y cell for 48 h, respectively. **a** Cell viability of SH-SY5Y cells was tested by CCK-8 assay. Inhibition of ERK1/2 activity using the PD98059 abolished the effect of P2Y2 overexpression on SH-SY5Y cell proliferation. **b**, **c** SH-SY5Y cell invasion was detected by Wound-healing assay. ATP enhanced the wound recovery ratio, which were inhibited by PD98059. **d**, **e** Transwell assay was used to examine SH-SY5Y cell migration. ATP promoted the SH-SY5Y cell migration, which was suppressed by PD98059. All experiments were performed in triplicate and presented as mean ± SE. $^{**}P < 0.01$ vs. Blank, $^{\#}P < 0.05$ vs ATP, $^{\#\#}P < 0.01$ vs ATP

### P2Y2 silencing suppresses the progression of HSCR in vivo

In addition, in vivo tumor growth assays were performed to further investigate the roles of P2Y2As shown in Fig. 5a, shRNA-P2Y2 significantly reduced the expression of P2Y2 in tumor tissues ($1.000 \pm 0.035$ vs. $0.248 \pm 0.009$, $P < 0.01$). Representative photographs of xenograft tumors (Fig. 5b) and quantification of tumor volume (Fig. 5c) are presented. Tumors showed a decrease in the P2Y2 silencing group relative to the control group (Fig. 5b, c, $487.737 \pm 50.868$ vs. $180.460 \pm 121.794$, $P < 0.01$). The phosphorylation level of ERK1/2 in tumor tissues was also decreased by shRNA-P2Y2 compared with that in the shRNA-NC group (Fig. 5d). Representative IHC images show the same results (Fig. 5e).

## Discussion

Hirschsprung disease (HSCR) is a congenital disorder affecting the enteric nervous system (Klein and Varga 2020). The occurrence of HSCR can be attributed to the migration, proliferation, and survival of ENCCs (Yu et al. 2021a). Our findings indicate a significant downregulation of P2Y2 expression in colon tissues affected by HSCR in comparison to its expression in normal colon tissues. This suggests a potentially essential role for P2Y2 in the development of the enteric neural crest. SH-SY5Y cells were selected for this study because of their accessibility, widespread usage, and origin from a neuroblast-derived extra-axial solid tumor of the neural crest. The present study suggests that P2Y2 silencing attenuates SH-SY5Y cell proliferation, migration, and invasion by suppressing the ERK1/2 signaling pathway.

The purinergic receptor P2Y2 is a G protein-coupled receptor that binds ATP to exert its action as a neurotransmitter (Zhang et al. 2012). Emerging evidence suggests that ATP and its receptors are involved in development and regeneration of the nervous system. A previous study using purine receptor agonists and inhibitors also demonstrated that ATP can promote outward axonal growth by binding to several receptors (Díaz-Hernandez et al. 2008). In neural stem cells, ATP and P2Y2 receptors promote the release of $Ca^{2+}$ from the endoplasmic reticulum by regulating the phosphatidylinositol-3 kinase signaling pathway, eventually promoting cell proliferation and differentiation (Ryu et al. 2003). ATP can also be released by the intestinal non-adrenergic non-cholinergic nerve (NANC) and functions as a vasoactive intestinal peptide and nitric oxide, two gastrointestinal NANC inhibitory neurotransmitters (Toda and Herman 2005; Mulè and Serio 2003). ATP and its receptors play significant roles in the development of ENS and intestinal peristalsis. Previous studies have shown that the mRNA expression levels of the P2Y2 receptor are significantly reduced in the distal rectum of rats with anorectal

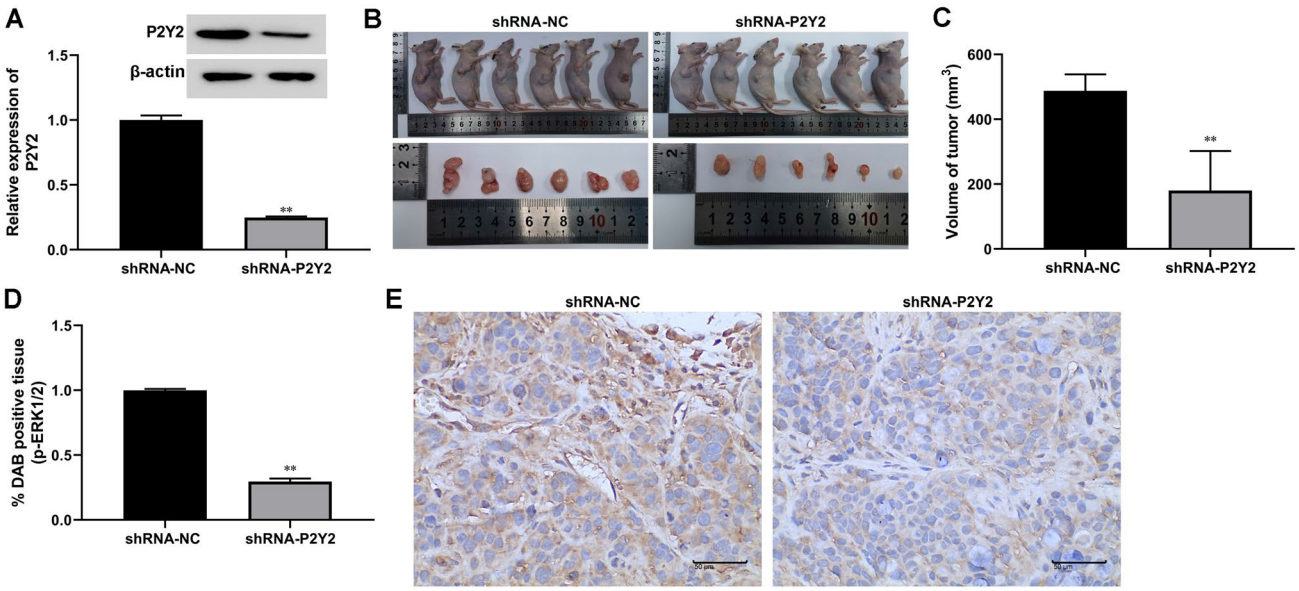


**Fig. 5** P2Y2 silencing suppressed the progression of HSCR in vivo. The xenograft model in vivo was generated by hypodermic injection of SH-SY5Y cells transfected with shRNA-P2Y2 into BALB/c nude mice for 21 days. **a** The expression of P2Y2 in tumor tissue was tested by Western blot. shRNA-P2Y2 reduced the expression of P2Y2 in tumor tissues. **b** Pictures of the tumors removed after 21 days. **c** The tumor volume was evaluated. The tumors showed a diminution in P2Y2 silencing group relative to control group. **d**, **e** Expression of p-ERK1/2 was measured by IHC assay in tumors. The positive immunohistochemical reaction was visualized as brown. The phosphorylation level of ERK1/2 in tumor tissues was also decreased by shRNA-P2Y2 compared with the shRNA-NC group. $^{**}P < 0.01$ vs. shRNA-NC

malformation (Liu et al. 2015; Zheng et al. 2019). Additionally, P2Y1 and P2Y2 receptors are markedly upregulated in the rectosigmoid mucosa of patients with diarrhea-predominant irritable bowel syndrome (Luo et al. 2016). More importantly, another study showed that the mRNA and protein expression levels of P2Y2 were both reduced in the aganglionic gut of embryos with HSCR, indicating that the P2Y2 receptor is associated with the development of ENS in HSCR embryos (Od and Puri 2008). The results of the present study showed that P2Y2 expression was downregulated in colon tissues of patients with HSCR. P2Y2 was significantly downregulated in dilated and stenotic segments of colon tissues compared to that in normal colon tissues. Additionally, the expression levels of P2Y2 were lower in the stenotic segment of the colon than in the dilated segment. Consistent with previous studies, the results of the current study also suggest that P2Y2 could play a significant role in the function of the central nervous system and the development of HSCR.

It has been suggested that alterations in the survival, proliferation, differentiation and migration of ENCCs can cause the lack of ganglion cells in the distal intestine, eventually promoting HSCR pathogenesis (Wang and Camilleri 2019; Meijers et al. 1992). Several genes such as RET (McKeown et al. 2013), NSD1 (Yu et al. 2021b), and WNT3A (Chen et al. 2014) have been reported to be markedly associated with ENCC proliferation and migration (McKeown et al. 2013). SH-SY5Y cells are often used to investigate the effect of P2Y2 on the development of ENCCs because of the difficulty in extracting and identifying ENCCs. MiR-195-5p inhibited the proliferation and invasion of SH-SY5Y cells in HSCR by targeting GFRA4 (Wang et al. 2021). Rac1/Limk1/Cofilin signaling pathway in HSCR regulates the proliferation and migration of SH-SY5Y cells, and this may be associated with the pathogenesis of HSCR (Zhou et al. 2022). lncRNA LOC100507600 functions as a competitive endogenous RNA to regulate BMI1 expression by sponging miR128-1-3p in HSCR (Su et al. 2018). Downregulation of LOC100507600 repressed SH-SY5Y cell migration and proliferation (Su et al. 2018). The present study demonstrated that P2Y2 silencing suppressed SH-SY5Y cell proliferation, migration, and invasion, which were all reversed following ATP-induced P2Y2 overexpression.

ERK1/2 is a member of the mitogen-activated protein kinase (MAPK) family, which plays a crucial role in regulating cell proliferation, differentiation, and apoptosis (Pearson et al. 2001). A previous study showed strong p-ERK activation in the colonic mucosa, enteric nervous system, and ENCCs of the normal colon (Corson et al. 2003; Rouleau et al. 2009). However, p-ERK staining was not observed in colon tissues derived from patients with HSCR (Rouleau et al. 2009). Another study revealed that MAPK/ERK1/2 signaling cascades could mediate the regulation of proliferation protein tyrosine phosphatase receptor-type R expression in ENCC overt differentiation and proliferation in HSCR (Tian et al. 2019). Additionally, inhibition of ERK1/2 activation reduced carbachol-induced contraction in innervated muscle strips, indicating that the ERK1/2 signaling pathway could play a critical role in gastrointestinal motility (Anderson et al. 2014). PD98059, a specific inhibitor of the ERK signaling pathway, selectively inhibits MEK1, a MAPK kinase, thereby inhibiting the phosphorylation of ERK1/2 (Hou et al. 2017; Zhao et al. 2017). Herein, treatment with PD98059 reversed the ATP-mediated enhanced proliferation, migration, and invasion abilities of SH-SY5Y cells, indicating that P2Y2 could regulate the development of HSCR by facilitating ERK1/2 activation.

Altogether, the current study identified the P2Y2/ERK1/2 pathway as the mechanism underlying SH-SY5Y cell proliferation, migration, and invasion in HSCR. Therefore, P2Y2 might be considered a novel and effective molecular target for treating HSCR. However, because of the limitations of this study, subsequent research should be validated in animal models of intestinal neural crest stem cells and HSCR.

**Acknowledgements** This study was supported by the Clinical Basic Research Project of Lanzhou University (no. ldyyyn2018-46), Gansu Provincial Department of Education Project/2020 Gansu Province Higher Education Innovation Ability Improvement Project (no. 2020B-002), and the Gansu Province Science and Technology Planning Project (no. 21JR1RA094).

**Data availability** The datasets used or analyzed during the current study are available from the corresponding author on reasonable request.

## Declarations

**Conflict of interest** The authors declare that they have no competing interests.

## References

Agresti C, Meomartini ME, Amadio S et al (2005) ATP regulates oligodendrocyte progenitor migration, proliferation, and differentiation: involvement of metabotropic P2 receptors. Brain Res Rev 48:157–165

Anderson CD Jr, Kendig DM, Al-Qudah M, Mahavadi S, Murthy KS, Grider JR (2014) Role of various kinases in muscarinic M3 receptor-mediated contraction of longitudinal muscle of rat colon. J Smooth Muscle Res 50:103–119

Bronner ME, Simões-Costa M (2016) The neural crest migrating into the twenty-first century. Curr Top Dev Biol 116:115–134

Burns AJ (2005) Migration of neural crest-derived enteric nervous system precursor cells to and within the gastrointestinal tract. Int J Dev Biol 49:143–150

Burnstock G (2007) Physiology and pathophysiology of purinergic neurotransmission. Physiol Rev 87:659–797

Chen D, Mi J, Liu X, Zhang J, Wang W, Gao H (2014) WNT3A gene expression is associated with isolated Hirschsprung disease polymorphism and disease status. Int J Clin Exp Pathol 7:1359–1368

Chen M, Chen H, Gu Y et al (2021) P2Y2 promotes fibroblasts activation and skeletal muscle fibrosis through AKT, ERK, and PKC. BMC Musculoskelet Disord 22:680

Corson LB, Yamanaka Y, Lai KM, Rossant J (2003) Spatial and temporal patterns of ERK signaling during mouse embryogenesis. Development 130:4527–4537

Díaz-Hernandez M, del Puerto A, Díaz-Hernandez JI et al (2008) Inhibition of the ATP-gated P2X7 receptor promotes axonal growth and branching in cultured hippocampal neurons. J Cell Sci 121:3717–3728

Fields RD (2011) Nonsynaptic and nonvesicular ATP release from neurons and relevance to neuron-glia signaling. Semin Cell Dev Biol 22:214–219

Hou L, Hou X, Wang L et al (2017) PD98059 impairs the cisplatin-resistance of ovarian cancer cells by suppressing ERK pathway and epithelial mesenchymal transition process. Cancer Biomark Sect A Dis Mark 21:187–194

Hu B, Cao L, Wang XY (2019) Downregulation of microRNA-431-5p promotes enteric neural crest cell proliferation via targeting LRSAM1 in Hirschsprung's disease. Dev Growth Differ 61:294–302

Kessmann J (2006) Hirschsprung's disease: diagnosis and management. Am Fam Physician 74:1319–1322

Klein M, Varga I (2020) Hirschsprung's disease-recent understanding of embryonic aspects, etiopathogenesis and future treatment avenues. Medicina (Kaunas) 56:611

Kudirka JC, Panupinthu N, Tesseyman MA, Dixon SJ, Bernier SM (2007) P2Y nucleotide receptor signaling through MAPK/ERK is regulated by extracellular matrix: involvement of beta3 integrins. J Cell Physiol 213:54–64

Lake JI, Heuckeroth RO (2013) Enteric nervous system development: migration, differentiation, and disease. Am J Physiol Gastrointest Liver Physiol 305:G1-24

Lalo U, Verkhratsky A, Pankratov Y (2011) Ionotropic ATP receptors in neuronal-glial communication. Semin Cell Dev Biol 22:220–228

Li C, Zhou Y, Rychahou P et al (2020) SIRT2 contributes to the regulation of intestinal cell proliferation and differentiation. Cell Mol Gastroenterol Hepatol 10:43–57

Liu YM, Kong M, Jin Z, Gao MM, Qu Y, Zheng ZB (2015) Expression of the P2Y2 receptor in the terminal rectum of fetal rats with anorectal malformation. Int J Clin Exp Med 8:1669–1676

Luo Y, Feng C, Wu J et al (2016) P2Y1, P2Y2, and TRPV1 receptors are increased in diarrhea-predominant irritable bowel syndrome and P2Y2 correlates with abdominal pain. Dig Dis Sci 61:2878–2886

McKeown SJ, Stamp L, Hao MM, Young HM (2013) Hirschsprung disease: a developmental disorder of the enteric nervous system. Wiley Interdiscip Rev Dev Biol 2:113–129

Meijers JH, van der Sanden MP, Tibboel D, van der Kamp AW, Luider TM, Molenaar JC (1992) Colonization characteristics of enteric neural crest cells: embryological aspects of Hirschsprung's disease. J Pediatr Surg 27:811–814

Mulè F, Serio R (2003) NANC inhibitory neurotransmission in mouse isolated stomach: involvement of nitric oxide, ATP and vasoactive intestinal polypeptide. Br J Pharmacol 140:431–437

Muscella A, Elia MG, Greco S, Storelli C, Marsigliante S (2003) Activation of P2Y2 receptor induces c-FOS protein through a pathway involving mitogen-activated protein kinases and phosphoinositide 3-kinases in HeLa cells. J Cell Physiol 195:234–240

O'Donnell AM, Puri P (2008) Deficiency of purinergic P2Y receptors in aganglionic intestine in Hirschsprung's disease. Pediatr Surg Int 24:77–80

Offenburger SL, Ho XY (2018) 6-OHDA-induced dopaminergic neurodegeneration in *Caenorhabditis elegans* is promoted by the engulfment pathway and inhibited by the transthyretin-related protein TTR-33. PLoS Genet 14:e1007125

Pan ZW, Li JC (2012) Advances in molecular genetics of Hirschsprung's disease. Anat Rec (Hoboken, NJ: 2007) 295:1628–1638

Pearson G, Robinson F, Beers Gibson T et al (2001) Mitogen-activated protein (MAP) kinase pathways: regulation and physiological functions. Endocr Rev 22:153–183

Rouleau C, Matécki S, Kalfa N, Costes V, de Santa BP (2009) Activation of MAP kinase (ERK1/2) in human neonatal colonic enteric nervous system. Neurogastroenterol Motil 21:207–214

Ryu JK, Choi HB, Hatori K et al (2003) Adenosine triphosphate induces proliferation of human neural stem cells: role of calcium and p70 ribosomal protein S6 kinase. J Neurosci Res 72:352–362

Su Y, Wen Z, Shen Q et al (2018) Long non-coding RNA LOC100507600 functions as a competitive endogenous RNA to regulate BMI1 expression by sponging miR128-1-3p in Hirschsprung's disease. Cell Cycle 17:459–467

Tam PK, Garcia-Barcelo M (2004) Molecular genetics of Hirschsprung's disease. Semin Pediatr Surg 13:236–248

Tian J, Zeng C, Tian Z et al (2019) Downregulation of protein tyrosine phosphatase receptor type R accounts for the progression of Hirschsprung disease. Front Mol Neurosci 12:92

Toda N, Herman AG (2005) Gastrointestinal function regulation by nitrergic efferent nerves. Pharmacol Rev 57:315–338

Wang XJ, Camilleri M (2019) Hirschsprung disease: insights on genes, penetrance, and prenatal diagnosis. Neurogastroenterol Motil 31:e13732

Wang G, Wang H, Zhang L, Guo F, Wu X, Liu Y (2021) MiR-195-5p inhibits proliferation and invasion of nerve cells in Hirschsprung disease by targeting GFRA4. Mol Cell Biochem 476:2061–2073

Yan J, Ma H, Lai X et al (2021) Artemisinin attenuated oxidative stress and apoptosis by inhibiting autophagy in MPP(+)-treated SH-SY5Y cells. J Biol Res (Thessalonike, Greece) 28:6

Yoneda A, Shima H, Nemeth L, Oue T, Puri P (2002) Selective chemical ablation of the enteric plexus in mice. Pediatr Surg Int 18:234–237

Yu Q, Du M, Zhang W et al (2021a) Mesenteric neural crest cells are the embryological basis of skip segment Hirschsprung's disease. Cell Mol Gastroenterol Hepatol 12:1–24

Yu XX, Chu X, Wu WJ et al (2021b) Common variation of the NSD1 gene is associated with susceptibility to Hirschsprung's disease in Chinese Han population. Pediatr Res 89:694–700

Zeng R, Huang J, Sun Y, Luo J (2020) Cell proliferation is induced in renal cell carcinoma through miR-92a-3p upregulation by targeting FBXW7. Oncol Lett 19:3258–3268

Zhang M, Piskuric NA, Vollmer C, Nurse CA (2012) P2Y2 receptor activation opens pannexin-1 channels in rat carotid body type II cells: potential role in amplifying the neurotransmitter ATP. J Physiol 590:4335–4350

Zhang S, Li J, He F, Wang XM (2015) Abnormal nuclear expression of Pygopus-2 in human primary hepatocellular carcinoma correlates with a poor prognosis. Histopathology 67:176–184

Zhao Y, Ge CC, Wang J et al (2017) MEK inhibitor, PD98059, promotes breast cancer cell migration by inducing β-catenin nuclear accumulation. Oncol Rep 38:3055–3063

Zheng Z, Chen B, Jin Z et al (2019) Downregulation of P2Y2 and HuD during the development of the enteric nervous system in fetal rats with anorectal malformations. Mol Med Rep 20:1297–1305

Zhou WK, Qu Y, Liu YM et al (2022) The abnormal phosphorylation of the Rac1, Lim-kinase 1, and Cofilin proteins in the pathogenesis of Hirschsprung's disease. Bioengineered 13:8548–8557